

## Smart self-cleaning coatings for corrosion protection

J. O. CARNEIRO, V. TEIXEIRA, S. AZEVEDO and  
M. MALTEZ-DA COSTA, University of Minho, Portugal

DOI: 10.1533/9780857096883.3.489

**Abstract:** Self-cleaning surfaces have attracted significant attention in recent years for their potential in both fundamental research and practical applications. Under the scope of self-cleaning smart coatings, this chapter explores the principal features of materials that can be used as protective coatings with an emphasis on the photocatalytic materials that have been developed to date. The chapter also highlights the importance of using titanium dioxide ( $\text{TiO}_2$ ) as a semiconductor material in industrial applications since it can act as a photoanode for metal cathodic protection.

**Key words:** titanium dioxide ( $\text{TiO}_2$ ), photocathodic corrosion protection, super-hydrophilicity, self-cleaning.

### 18.1 Introduction

Corrosion is a naturally occurring phenomenon that causes substantial damage to materials and equipment such as automobiles, airplanes, steel bridges, and energy production and distribution systems. According to a NACE report in 1998, the cost of corrosion control in the US alone was 276 billion dollars. In 2011 this cost was estimated to have risen to over 1 trillion dollars, representing a huge cost to the US economy (Hays, 2012). The most common methods used for corrosion prevention and control include (NACE, 2002):

- organic and metallic protective coatings;
- corrosion-resistant alloys, plastics and polymers;
- corrosion inhibitors;
- cathodic protection.

These methods can be expensive; however, more and new cost-effective methods for preventing corrosion are needed. Protective coatings are by far the most usual and effective method of corrosion prevention. The main purpose of protective coatings is to provide an anti-corrosion barrier between the structural material and the corrosive environment. The most established strategies involve the application of paint films, sealers, similar

polymer-based materials or specially designed chemicals such as surfactants, in order to obtain an effective isolation barrier that will remain adhered to the surface in the presence of a corrosive environment (Dickie and Floyd, 1986).

Recent advances in nanotechnology, more specifically in the materials field, have led to the research and implementation of new coating materials with interesting features in terms of corrosion control and prevention. Nanomaterials have unique mechanical, electrical, optical and reactive properties, which are distinct from bulk materials and which provide them with the ability to incorporate new coating formulations and thereby add value to the final material. Procedures for producing coating materials with chemically resistant nanofilms or oxides have received significant attention in recent years. Some formulations of coatings, which incorporate nanofilms and nanoparticles, are currently available on the market and are used in industrial applications. The leading current applications of nanotechnology are as nanocoatings for insulating, self-cleaning, UV protection, corrosion resistance and waterproofing. Many of these coatings incorporate titanium dioxide ( $\text{TiO}_2$ ) nanoparticles to create self-cleaning surfaces that are also able to remove pollutants from the surrounding environment. The existing nanotechnology could potentially considerably decrease industrial costs, in areas such as corrosion prevention and control, but the lack of awareness, training and competent personnel, along with the current over-reliance on standard industrial practices and general resistance to new technology and solutions continue to be obstacles to its effective implementation.

Smart materials/coatings is a relatively new name for materials and products that are capable of changing their properties in response to physical and/or chemical influences such as light, temperature or the application of an electric field. The smart coatings developed to date can be categorized in various ways, i.e. according to their functional ingredients, application, fabrication methods, etc. For example, smart coatings categorized according to their stimuli/response qualities include: coatings acting as sensors; coatings that respond to changes in light, heat or pressure; corrosion control coatings; command-destruct coatings; and colour shifting coatings. Bioactive coatings include: hygienic, antifouling, biodecontamination/detection and biocatalytic coatings. Other types of smart coatings, which are more difficult to classify, include: self-assembling polymers/coatings, electrically conducting coatings, super-insulating coatings, self-repair and self-healing coatings, super-hydrophobic coatings, self-lubricating coatings, molecular brushes and optically active coatings.

Of the huge range of existing smart coatings, it is those with self-cleaning surfaces that attract the most attention for their potential uses in both fundamental research and practical applications. So far, self-cleaning has been demonstrated using the following four approaches: the  $\text{TiO}_2$ -based

self-cleaning that arises from photo-induced super-hydrophilicity and from photocatalysis; the lotus self-cleaning effect (super-hydrophobicity with a small sliding angle) in which dirt particles can be removed by water droplets; the gecko setae-inspired dry self-cleaning in which particles are removed without using liquids; and the underwater organism inspired antifouling self-cleaning, which uses surfaces with special chemical and physical structures (Liu and Jiang, 2012). The advantages of self-cleaning coatings range from reducing maintenance costs and the prevention of snow and ice build-up to protection from environmental pollution. The present variety of practical application fields include: textiles (self-cleaning clothes), automotive (glazing, car bodies, lamp covers and mirrors), building (glazing, facades, doors and window profiles, plastic roofs), agriculture (greenhouse covers), household (bathrooms, kitchen fittings), optical applications (cameras, lenses, optical sensors), marine applications (anti-corrosion protection) and aerospace (non-stick and ice phobic surfaces). Consequently, a great deal of effort has been directed towards the commercial development of self-cleaning applications (Challener, 2006). Since Fujishima and Honda (1972) reported the water splitting reaction that occurs at a  $\text{TiO}_2$  electrode's surface when it is being irradiated with UV light, the coatings have been applied to a varied range of surfaces.

Under the scope of self-cleaning smart coatings, this chapter will explore the principal features of materials that can be used as protective coatings with an emphasis on photocatalytic materials. Semiconductor materials, such as  $\text{TiO}_2$ , zinc oxide ( $\text{ZnO}$ ), tungsten oxide ( $\text{WO}_3$ ) and cadmium selenide ( $\text{CdSe}$ ), are all examples of self-cleaning smart coatings, but this chapter will highlight  $\text{TiO}_2$ -based materials, because they are the most widely studied, and will particularly focus on doped  $\text{TiO}_2$  materials since it has been reported that the addition of dopants can significantly enhance the performance of the  $\text{TiO}_2$  catalyst (Teh and Mohamed, 2011). Characteristics such as low toxicity, high chemical stability, availability and low cost, in addition to the self-cleaning and anti-corrosion properties, make  $\text{TiO}_2$  the ideal candidate for industrial purposes. Moreover, when used in corrosion protection applications,  $\text{TiO}_2$  did not exhibit the disadvantages that other sacrificial materials (such as Mg) do, when applied to the cathodic protection process. This means that, unlike other sacrificial materials,  $\text{TiO}_2$  would not need to be replaced after a certain period due to its degradation.

## 18.2 Types of self-cleaning coatings

The development of nanoengineered surfaces has been leading to the production of smart, self-cleaning coatings with tailored surface properties. The traditional surface cleaning of materials can cause considerable difficulties because it requires the use of chemical detergents, consumes

large amounts of energy and, consequently, generates high costs. The main method of achieving self-cleaning surfaces is through the development of either hydrophilic or hydrophobic surfaces. Surface wettability is generally evaluated using the water contact angle (CA), which is defined as the angle between the solid surface and the tangent line of the liquid phase at the interface of the solid–liquid–gas phases. Initially, a TiO<sub>2</sub> thin film exhibits a CA of several tens of degrees, depending on the roughness of the surface conditions. When this surface is exposed to UV light, the CA of the water decreases (reaching almost 0°), because the water tends to spread out flat. At this phase, the surface becomes completely non-water-repellent and is called ‘super-hydrophilic.’ At the other end of the scale, a CA of 180° corresponds to complete non-wetting, known as a ‘super-hydrophobic’ surface. According to some authors, when a TiO<sub>2</sub> surface is irradiated with UV light a completely clean surface can be obtained through a photocatalytic reaction and due to some structural changes, which cause a highly hydrophilic state (Hashimoto *et al.*, 2005).

In 1805, Young reported research work related to the discovery of the basic law in determining the equilibrium shape of a liquid drop on a surface (Young, 1805). The well-known Young’s equation can be written as follows:

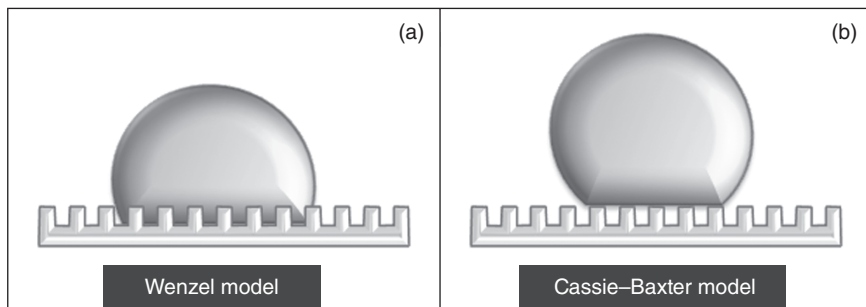
$$\gamma_{sg} = \gamma_{sl} + \gamma_{lg} \cos \theta_Y \quad [18.1]$$

where  $\theta_Y$  is the Young contact angle (between a water droplet and a solid surface) and  $\gamma_{sg}$ ,  $\gamma_{sl}$  and  $\gamma_{lg}$  refers to the interfacial surface tensions of solid, liquid and gas, respectively. The contact angle results from the thermodynamic equilibrium of free energy at the solid–liquid–gas interface. This equation does not, however, consider the influence of certain parameters such as chemical heterogeneity or roughness. Solid surfaces do not fulfil this ideal situation yet surface roughness was considered to be a parameter that substantially influences the contact angles and one that should, consequently, be taken into account when surface wettability is being evaluated. In fact, two models were developed in order to correlate the obtained surface contact angles with its roughness: the Wenzel and the Cassie–Baxter models (see Fig. 18.1).

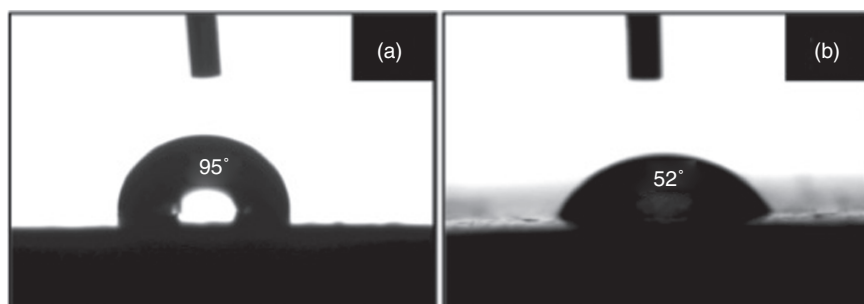
In 1936 Wenzel described a model that clarified the influence of roughness in the contact angle with the following equation:

$$\cos \theta_W = r \cos \theta_Y \quad [18.2]$$

where  $\theta_W$  is the apparent contact angle in the Wenzel model,  $\theta_Y$  is the Young’s contact angle and  $r$  is the surface roughness factor given by the ratio of rough to planar surface areas. This model assumes that surface roughness enhances the wettability and, therefore, accounts for the nature of the corresponding flat surface (Quéré, 2008). For cases in which  $r$  is greater than 1, a given hydrophobic surface ( $\theta_Y > 90^\circ$ ) becomes more hydrophobic



18.1 Schematic representation of (a) Wenzel and (b) Cassie-Baxter models.



18.2 Images displaying the water droplet on top of (a) ceramic substrate coated with  $\text{TiO}_2$  thin film and (b) ceramic substrate coated with a polymeric layer containing  $\text{TiO}_2$  nanoparticles.

( $\theta_w > \theta_Y$ ) when rougher and a hydrophilic surface ( $\theta_Y < 90^\circ$ ) becomes even more hydrophilic ( $\theta_w < \theta_Y$ ). In the majority of the cases these conditions do occur, but the model presented by Wenzel is not satisfactory when the sample surface exhibits a chemical heterogeneous behaviour. Taking this situation into account, Cassie and Baxter (1944) derived an equation with which is possible to describe the influence of chemical heterogeneities on the contact angle between a water droplet and a solid surface.

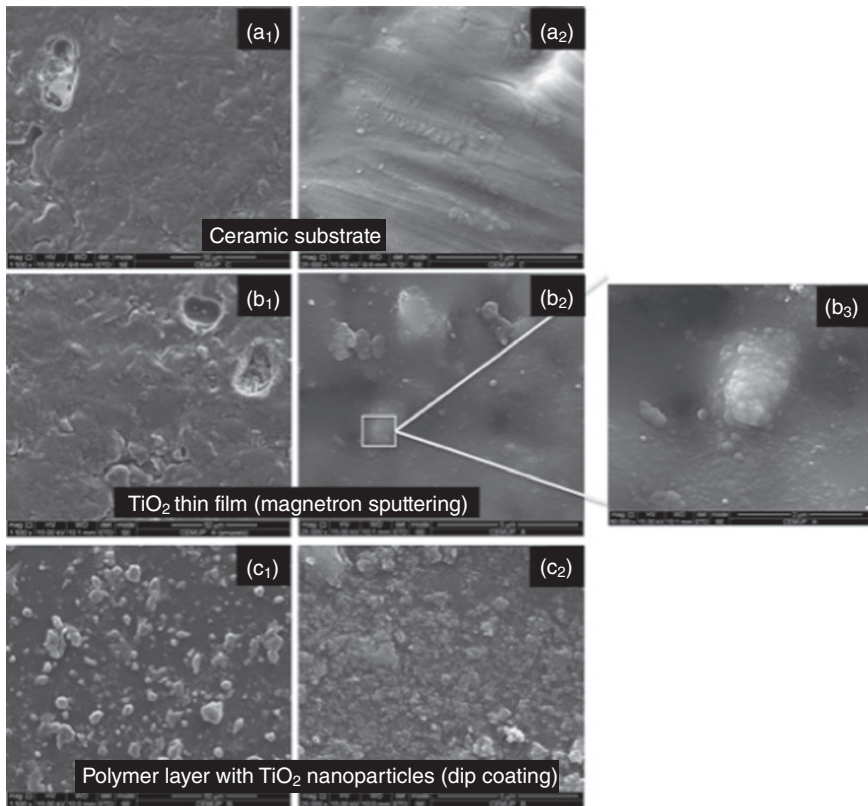
In cases where only air is present between the solid surface and the liquid, the cosine of the angle is  $-1$ . The Cassie-Baxter equation can, therefore, be written as follows:

$$\cos \theta_{CB} = [f_s (\cos \theta_Y + 1) - 1] \quad [18.3]$$

where  $\theta_{CB}$  is the apparent contact angle in the Cassie-Baxter model and  $f_s$  is the surface fraction of the solid. For example, Fig. 18.2 shows images of a water droplet on the top of coated ceramic substrates with  $\text{TiO}_2$ -based

materials in the form of thin film (Fig. 18.2a) and a polymeric layer containing TiO<sub>2</sub> nanoparticles (Fig. 18.2b). The contact angles of the ceramic substrates coated with TiO<sub>2</sub> thin films and the TiO<sub>2</sub> nanoparticles are 95° (hydrophobic surface) and 52° (hydrophilic surface), respectively. A possible reason for the different hydrophilic and hydrophobic behaviour presented by the coated substrates could be their dissimilar surface roughness. According to Hashimoto *et al.* (2005), the roughness on the surface of a sample enhances the hydrophilic state of that surface.

Figure 18.3 shows the different top-views of scanning electron microscopy (SEM) micrographs of the coated samples as well as the surface aspect of the bare ceramic substrate. In fact, from the observation of these SEM micrographs (b<sub>1</sub> to c<sub>2</sub>) it is clear that the ceramic substrate coated with the



18.3 Top-view SEM micrographs of (a) bare ceramic substrate, (b) TiO<sub>2</sub> thin film deposited by DC magnetron sputtering and (c) polymeric layer containing TiO<sub>2</sub> nanoparticles. The subscripts 1, 2 and 3 refers to different magnifications, namely 1500×, 25000× and 50000×, respectively.

polymeric layer containing  $\text{TiO}_2$  (e.g. Fig. 18.3c<sub>2</sub>) has a rougher surface than the  $\text{TiO}_2$  thin film (e.g. Fig. 18.3b<sub>2</sub>).

An evaluation of Fig. 18.3a<sub>1</sub> clearly shows the rough and highly porous surface of the ceramic substrate. Under a high magnification (Fig. 18.3a<sub>2</sub>) it is also possible to see that the polish process, used by the company to improve the aesthetic appearance of the substrates, resulted in the presence of dip scratches and some material sliding. In Fig. 18.3b<sub>1</sub> and 18.3b<sub>2</sub> it is possible to evaluate the surface morphology of the  $\text{TiO}_2$  thin film deposited by DC magnetron sputtering. At a low magnification the only conclusion that can be drawn is that the thin film is copying the morphology of the ceramic substrate. In Fig. 18.3b<sub>3</sub>, however, it is possible to perceive the presence of the  $\text{TiO}_2$  thin film, which reveals a randomly oriented structure. The  $\text{TiO}_2$  polymeric layers containing  $\text{TiO}_2$  nanoparticles have a more porous surface structure, which can eventually lead to enhanced photocatalytic activity due to the larger activation area (Perkgoz *et al.*, 2011) as can be seen in Fig. 18.3c. It can also be inferred from these results that  $\text{TiO}_2$  nanoparticles tend to form agglomerates. In accordance with Vero *et al.* (2009), reducing van der Waals forces and increasing repulsive Coulomb interactions can control the nanoparticle's agglomeration. In fact, pure  $\text{TiO}_2$  has its isoelectric point (IEP) at pH values in between 4.5 and 6.5 (Furlong and Sing, 1979; Winkler, 2003). Since the  $\text{TiO}_2$  aqueous solution used in this experimental work was prepared at a pH = 4.98, we believe that van der Waals forces are mainly responsible for the agglomeration of the  $\text{TiO}_2$  nanoparticles used.

The photocatalytic properties of  $\text{TiO}_2$  materials (Carneiro *et al.*, 2012) are responsible for the change of the contact angle between a water droplet and a given solid material, which may lead to a more hydrophobic (super-hydrophobic when  $\theta > 120^\circ$ ) or hydrophilic (super-hydrophilic when  $\theta$  is nearly  $0^\circ$ ) surface and increase its self-cleaning ability. Additionally, in 1990, Fujishima discovered that the wettability of  $\text{TiO}_2$  changes before and after UV irradiation exposure, which clearly enhanced the application range of this semiconductor material. The outstanding properties of  $\text{TiO}_2$  materials triggered a huge interest in this new class of surfaces (and coatings) since they can find applications in a variety of markets including water-repellents, snow and anti-ice products, anti-fogging windows, screens and lenses, and foils for food packaging. The importance of this sub-area of surface chemistry can also be related to the cost-effective fabrication technologies used to produce super-hydrophilic and super-hydrophobic surfaces.

### 18.3 Techniques for developing self-cleaning coatings

Self-cleaning coatings can be deposited using a number of different techniques on a variety of substrates including glass, polymers, textiles,

metals and ceramics. Many studies have been conducted into the possibility of also producing  $\text{TiO}_2$  thin films using a variety of deposition techniques such as plasma enhanced chemical vapour deposition (PECVD) (Szymanowski *et al.*, 2005), sol–gel methods on cotton, wool and polyethylene terephthalate (Dong *et al.*, 2006; Fei *et al.*, 2006; Xu *et al.*, 2006; Qi *et al.*, 2007; Uddin *et al.*, 2007; Yuranova *et al.*, 2007; Tung and Daoud, 2009), liquid phase deposition on carbon fibres (Herbig and Löbmann, 2004), DC magnetron sputtering on polyester nonwoven (Xu *et al.*, 2008) and radio frequency (RF) sputtering on polypropylene fibres (Wei *et al.*, 2007). Low temperature synthesis, however, has proven to be the most suitable process for temperature-sensitive substrate materials. Of the deposition methods studied, pulsed DC magnetron sputtering (PMS) has attracted particular interest in the sputtering field, since it can be used, at low substrate temperature, to prepare high quality thin films with high density, strong adhesion, improved hardness, better transparency and a good uniformity over large areas, because the process reduces or eliminates arcs during the deposition process (Carneiro *et al.*, 2005, 2007, 2008).

From a practical application point of view, the development of crystalline  $\text{TiO}_2$  layers at room temperature is essential. The produced  $\text{TiO}_2$  coatings are generally amorphous, however, meaning that they require further heat treatments at relatively high temperatures. Sol–gel-based techniques have recently been pointed out as promising techniques for the preparation of high quality coatings containing  $\text{TiO}_2$  nanoparticles for smart self-cleaning applications. Additionally, the deposited thin film's microstructure produced using sol-gel methods, i.e. pore size, pore volume and surface area, can be tailored by combining the adequate process conditions (Brinker and Schere, 1990). The existence of cracks and defects on the coating's surfaces can lead to an appearance of local corrosion that can be avoided by using specific protective thin films or coatings such as a  $\text{TiO}_2$  semiconductor material, which will be explained in some detail in the next section (Gluszek *et al.*, 1990; Shanaghi *et al.*, 2009).

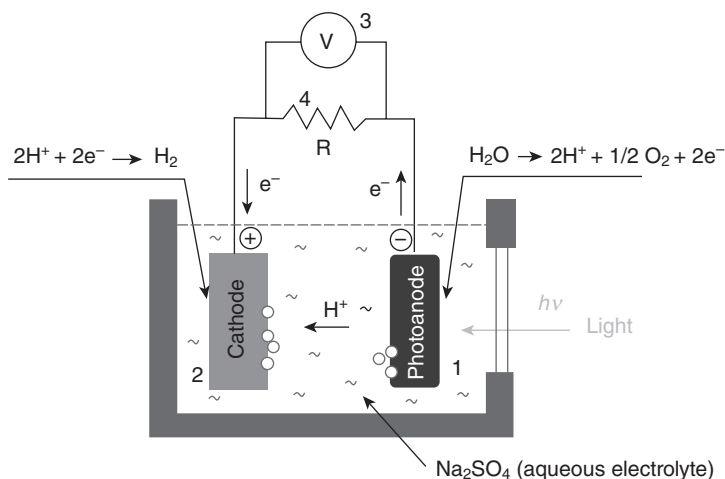
## 18.4 $\text{TiO}_2$ as a material for corrosion protection

This section introduces the basic mechanism of photo-electrolysis promoted by a suitable photocatalyst (the  $\text{TiO}_2$  semiconductor) for splitting water molecules into hydrogen and oxygen. In addition, the application of a  $\text{TiO}_2$  semiconductor in photo-electrochemistry for the purpose of metal corrosion prevention will be presented. Since the first article by Fujishima and Honda in 1972, many research groups have investigated the photocatalytic splitting of water into hydrogen and oxygen under the influence of light.

18.4.1 Water photo-electrolysis promoted by  $\text{TiO}_2$ 

A very important method of converting sunlight into hydrogen is through the photo-electrolysis of water, which uses photo-electrochemical light collecting systems (PEC) to power the electrolysis of water. Figure 18.4 shows a schematic of a single PEC proposed by Fujishima and Honda (1972).

During the water electrolysis process  $\text{H}_2\text{O}$  is broken down into hydrogen and oxygen gas. Electrolytes dissolve and dissociate into cations and anions that carry the current. This process can occur in an electrolysis cell, which consists of two electrodes: a cathode and an anode, in which reduction and oxidation reactions occur simultaneously forming  $\text{H}_2$  (at the cathode) and  $\text{O}_2$  (at the anode). Photo-electrolysis can be carried out in an electrolysis cell where, in its configuration, one of the two electrodes is formed by a semiconductor material (see Fig. 18.4). Upon exposure to sunlight the semiconductor electrode, called a photo-electrode, immersed in an aqueous electrolyte solution, generates (in an ideal case) enough electrical energy to drive the respective oxygen and hydrogen evolution reactions at the interfaces of the photoanode and cathode within the electrolyte. A necessary condition for such a spontaneous water splitting process upon irradiation is that the edge of the semiconductor conduction band should lie in a more negative position (see standard hydrogen electrode, – SHE, as reference) relative to the reduction potential of the water. The edge of the valence

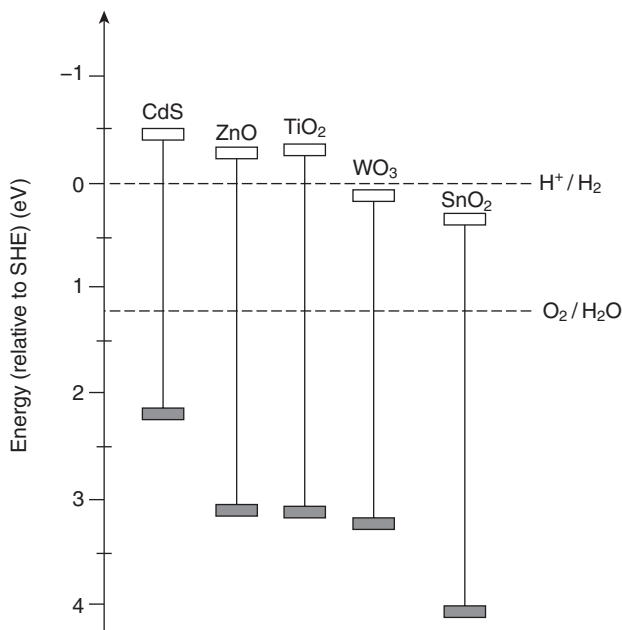


18.4 Schematic diagram of solar photo-electrolysis: (1) photoanode electrode; (2) cathode counter electrode; (3) voltmeter; and (4) load resistance.

band, meanwhile, should be more positive than the oxidation potential. Photo-electrolysis integrates solar energy absorption and water electrolysis into a single photo-electrode. This method does not require a separate power generator.

Semiconductors can absorb light with energy higher than the energy threshold determined by their band gaps. Once photons are absorbed, photo-electrons and photo-holes are formed. The photo-generated electrons and holes quickly relax to the bottom of the conduction band and the top of the valence band respectively by dissipating their kinetic energy. These electrons and holes can be used to drive a redox reaction. Thermodynamically the energy level of the conduction band (CB) edge is a measure of the reduction strength of the electron in the semiconductor, whereas valence band (VB) edge is a measure of the oxidation power of holes in the semiconductor (Hoffmann *et al.*, 1995). Figure 18.5 shows band edge energy levels of common semiconductors that are in contact with an aqueous medium (Serpone, 1995; Grätzel, 2001).

For semiconductors to be suitable to work as photoanodes for solar water photo-electrolysis they must have the following general properties (Grimes *et al.*, 2007):



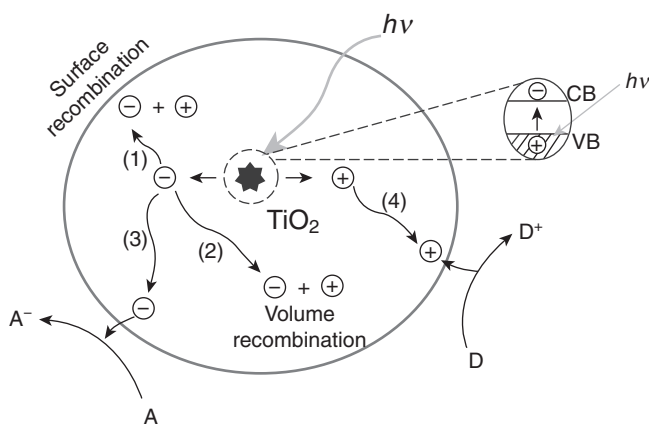
18.5 Band positions (top of valence band and bottom of conduction band) of several semiconductors together with some selected redox potentials. Figure adapted from Grätzel (2001) and Grimes *et al.* (2007).

- chemical stability both under illumination and in the dark;
- a band gap of about 2.0 eV to absorb maximum solar radiation;
- scarcity of electron/hole charge recombination to prevent the recombination of the photo-generated charge carriers;
- suitable band edge positioning with respect to the  $H^+/H_2$  reduction potential and  $O_2/OH^-$  oxidation potential.

There are many semiconductors that possess one of the above properties.  $TiO_2$ , however, is one of the most promising candidates for use as a commercial photo-electrode in a photo-electrochemical cell for the production of solar-hydrogen, for the following reasons:

- Good chemical/photochemical stability and high oxidation power ( $E = 3.2\text{ eV}$  vs SHE).
- $TiO_2$  exhibits exceptional resistance to corrosion and photo-corrosion in aqueous environments (Reiche, 1950).
- $TiO_2$  is reactive with both light and water (Nowotny *et al.*, 2005).
- $TiO_2$  is substantially less expensive than other photosensitive materials.
- $TiO_2$  with enhanced photosensitivity has many supplementary applications that are environmentally friendly (Fujishima *et al.*, 1999).
- $TiO_2$  is abundant in the Earth's crust.

Figure 18.6 shows a schematic representation of the photo-excitation of a  $TiO_2$  solid particle through exposure to radiation with energy above the band gap energy. An excitation, produced by the absorption of a photon (represented by the star symbol), is followed by charge separation – causing the production of electron/hole pairs.



18.6 Schematic photo-excitation in a  $TiO_2$  semiconductor particle followed by later events. Figure adapted from Linsebigler *et al.* (1995).

Processes (1) and (2) represent electron/hole pair recombination processes at the surface and in the bulk, respectively. The electron/hole charge transport to the particle surface through processes (3) and (4), respectively lead to desirable reduction and oxidation reactions at the surface. Herein, A represents electron acceptor species (i.e. A is reduced by electrons that migrates to the particle surface) whereas D denotes species that are electron donors (D is oxidized by migrating holes).

In the pioneering work of Fujishima and Honda (1972), the UV light irradiation of a TiO<sub>2</sub> photo-electrode in aqueous solution led to the production of H<sub>2</sub> and O<sub>2</sub> on a Pt counter-electrode and a TiO<sub>2</sub> photo-electrode, respectively. When the surface of the TiO<sub>2</sub> semiconductor photo-electrode was irradiated with light, consisting of wavelengths shorter than its band gap (about 415 nm or 3.0 eV for the rutile crystalline phase), photocurrent flowed from the platinum counter-electrode to the TiO<sub>2</sub> electrode through the external circuit. The direction of the current revealed that the oxidation reaction (oxygen gas evolution) appears at the TiO<sub>2</sub> photo-electrode and the reduction reaction (hydrogen evolution) at the Pt electrode. This observation showed that water could be broken down, using UV light, into O<sub>2</sub> and H<sub>2</sub>, without the use of an external power generator, according to the following reactions:

- At the TiO<sub>2</sub> photo-electrode:



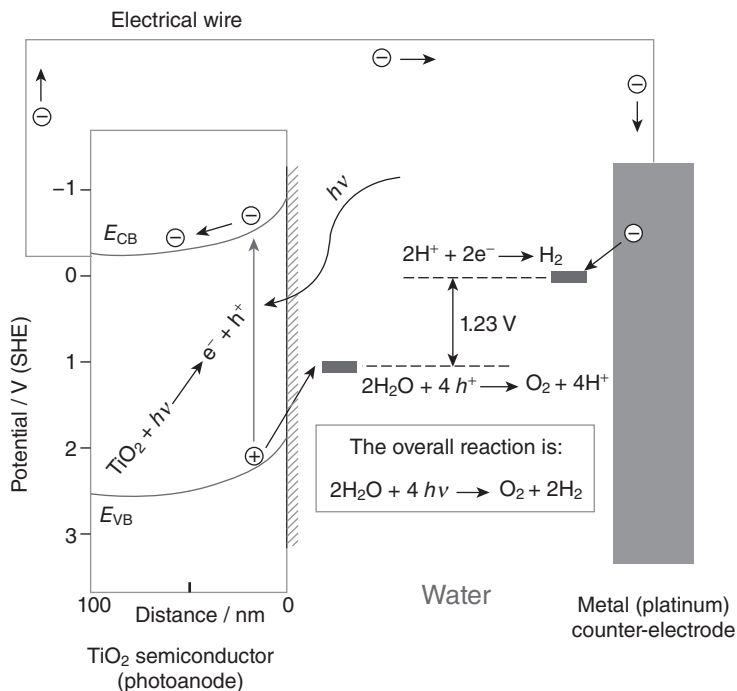
- At the Pt electrode:



Figure 18.7 depicts the band energy scheme of this reaction.

When a semiconductor electrode is in contact with an electrolyte solution, thermodynamic equilibration occurs at the interface. This may result in the creation of a space-charge layer within a thin surface region of the semiconductor, in which the electronic energy bands are bent upwards in the case of n-type semiconductors. For the n-type semiconductor, the electric field existing across the space-charge layer drives photo-generated holes toward the interfacial region (solid/liquid) and electrons toward the interior of the electrode and from there to the electrical connection of the external circuit.

If the conduction band energy  $E_{\text{CB}}$  is more negative (on the electrochemical scale) than the hydrogen evolution potential, photo-generated electrons can flow to the counter-electrode and reduce protons, resulting in a hydrogen gas evolution without an applied potential. The TiO<sub>2</sub> semiconductor material fulfils this requirement. In fact, when semiconductor electrodes are used as either photoanodes or photocathodes for water electrolysis, the energy

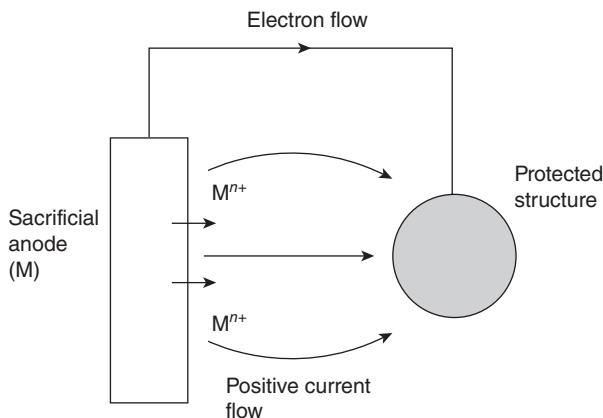


18.7 Energy band diagram of photo-electrochemical water electrolysis promoted by the TiO<sub>2</sub> semiconductor electrode illuminated by UV light. Figure adapted from Hashimoto *et al.* (2005).

band gap should be at least 1.23 eV (the equilibrium cell potential energy for water electrolysis at 25 °C and 1 atm).

#### 18.4.2 Metal corrosion protection

Corrosion is a major warning about the integrity of infrastructures such as buildings, steel bridges, onshore and offshore plants and transport pipelines. Cathodic protection is the most common technique used to mitigate corrosion and involves changing the potential of the corroding metal by pumping in electrons (Jones, 1996). There are two principal conventional methods of applying cathodic protection: the impressed-current technique and the use of sacrificial anodes. The former includes the structure as part of a driven electrochemical cell and the latter includes the structure as part of a spontaneous galvanic cell. In the impressed-current technique the driven voltage for the protective current comes from a DC power source. The sacrificial anode technique uses the natural potential difference that exists between the structure and a second metal in the same environment to

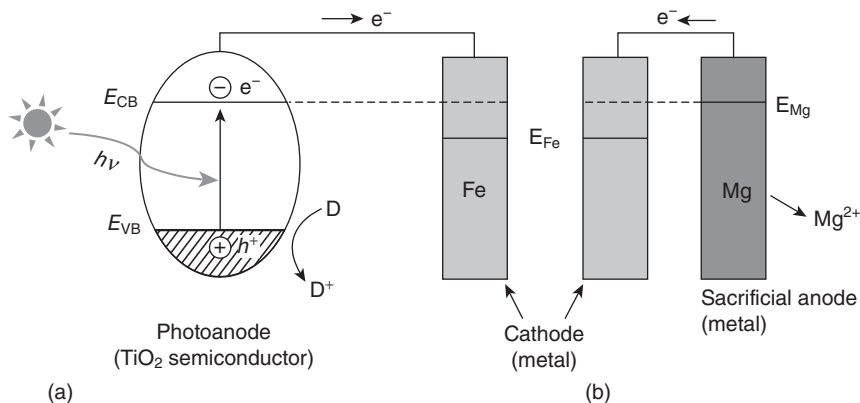


**18.8** Schematic diagram of conventional cathodic protection using sacrificial anodes. The electrons generated from the corroding sacrificial anode are transferred to the metal object to reduce its corrosion rate.

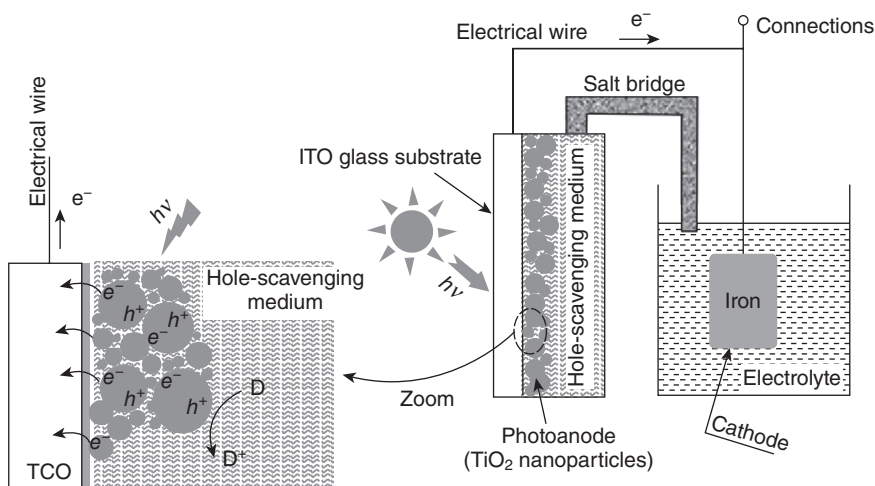
provide the driving voltage. In this latter technique, no power source is employed and the dissolution of the second metal, the sacrificial anode, provides the source of electrons for the cathodic polarization of the structure. The impressed-current anode may be nobler than the protected structure (because the power source forces it to act as an anode) but, the sacrificial anode must be spontaneously anodic to the structure, i.e. be more negative in the galvanic series for the given environment. Thus, in principle, magnesium, zinc or aluminium could be used to protect steel, and iron to protect copper. Figure 18.8 illustrates the use of a sacrificial anode for conventional cathodic protection.

With the emergence of nanotechnology and the increasing demand for environmentally friendly technology, intense research has been undertaken to study the viability of using semiconductor materials to improve corrosion protection. Several researchers have suggested the use of the photo-electrochemical technique in the corrosion prevention of steel (Moussa and Hocking, 2001; Ohko *et al.*, 2001). Recent studies have shown that the cathodic protection of steel promoted by UV irradiated  $\text{TiO}_2$  nanoparticles is a highly promising technique. The technique offers a galvanic system without anode consumption. The central idea is to replace the conventional sacrificial anodes (such as Mg, Zn or Al) with the  $\text{TiO}_2$  semiconductor photoanode, which, under light irradiation, can generate electrons at the CB and then pump those electrons in the corroding metal (see Fig. 18.9).

The work performed by Park *et al.* (2001) is very interesting. Corrosion prevention experiments were carried out with a photo-electrochemical set-up consisting of a flat solar panel containing  $\text{TiO}_2$  nanoparticles (acting



18.9 Schematic representation of metal (Fe) corrosion protection using (a) a  $\text{TiO}_2$  photoanode where D denotes hole-scavengers while dashed lines represent the electrochemical potential of the electrons generated in the photoanode and (b) a conventional sacrificial metallic anode (e.g. Mg).

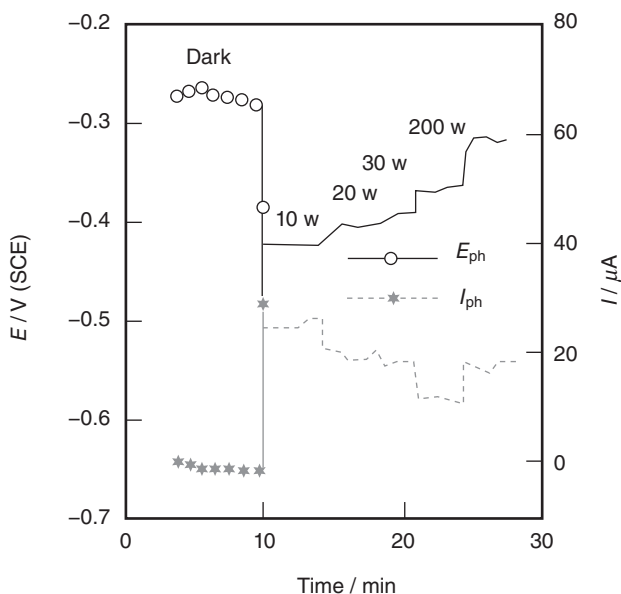


18.10 Schematic diagram of an electrochemical photocell using as photoanode  $\text{TiO}_2$  nanoparticles deposited on an indium tin oxide (ITO) coated glass substrate.

as the photoanode) in a hole-scavenging medium and a steel electrode that had been immersed in an  $0.05\text{M K}_2\text{CO}_3$  aqueous solution at pH 4 (see Fig. 18.10).

A semiconductor photoanode was prepared by applying a  $\text{TiO}_2$  (Degussa P25) suspension (5 wt%) to an indium tin oxide (ITO) coated glass substrate, which was then annealed at  $450^\circ\text{C}$  for 30 min. Indium tin oxide thin film is

the transparent conducting oxide (TCO) most widely used for display applications and photovoltaic (PV) devices, where it acts as both an electrode element and a structural template (Fortunato *et al.*, 2007). In the work developed by Park *et al.* the  $\text{TiO}_2/\text{ITO}$  electrode was placed in a solid-phase hole-scavenging medium (sodium formate salt) and encased in a transparent Petri dish to form a flat solar cell. The  $\text{TiO}_2/\text{ITO}$  electrode and the steel electrode were galvanically coupled through an external circuit (the electrical contact was made by attaching a copper wire with silver paste at the uncoated edge of the ITO glass substrate) and the two cells were connected via a salt bridge (saturated KCl in agar). In order to excite the  $\text{TiO}_2$  photoanode (illuminated from the ITO side), they used different light sources, namely a 200W mercury lamp and 10W blacklight lamps (one, two and three lamps for 10, 20 and 30W illumination, respectively). The corroded steel surface was analysed by a Raman spectroscopy for different illumination conditions: sample continuously illuminated (30W lamp); sample in open air and exposed to sunlight illumination (16h plus 14h in dark) and a control sample not connected to the photoanode. Figure 18.11 shows the change in potentials and currents during the galvanic coupling of the  $\text{TiO}_2$  photoanode, when the steel electrode was placed in acidic water

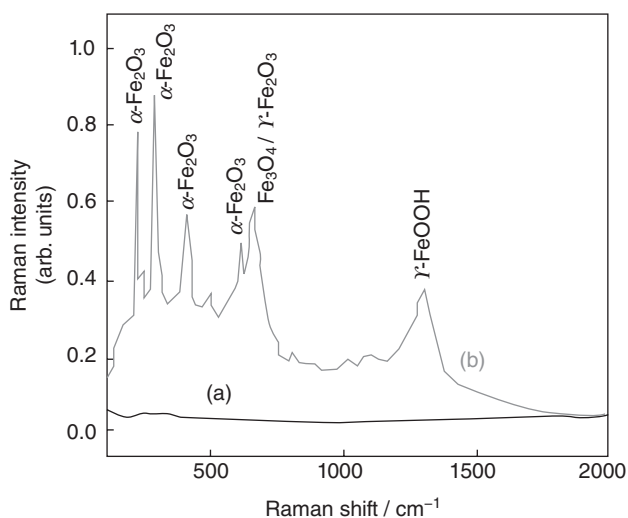


18.11 The change of  $E_{ph}$  and  $I_{ph}$  in the galvanic couple of a  $\text{TiO}_2$  photoanode and the steel electrode under a photoanode irradiated by 10, 20, 30 or 200W lamp or solar light. Figure adapted from Park *et al.* (2001).

(pH 4) and when the photoanode was irradiated under different sources of light.

Under illumination conditions, the coupled photo-potential,  $E_{ph}$ , suddenly shifted to a more negative potential with a concomitant increase of photocurrent,  $I_{ph}$ . In addition, the measured open circuit potential ( $E_{oc}$ ) of the  $TiO_2$  photoanode, under a 30W light illumination, was 20.9V (vs. standard calomel electrode, SCE). When comparing this value with the  $E_{oc}$  of the steel electrode (20.44V vs. SCE), it is possible to conclude that the illuminated  $TiO_2$  photoanode supplied CB electrons to the metal electrode, and therefore promoted cathodic protection. In this experimental work the authors also observed that the surface of the steel electrode, in the control sample that was not connected to the photoanode, quickly corroded and was covered by red-brown rust. They also used Raman spectroscopy to quantify the evolution of corrosion on the steel surfaces. Figure 18.12 compares the Raman spectra of the steel surface corroded in a 0.05 M  $K_2CO_3$  acidic solution under illumination conditions. All the detected peaks were assigned to various phases of iron oxides (Oblonsky and Devine, 1995).

From Fig. 18.12 one can observe that the steel surface connected to a continuously illuminated photoanode does not show iron oxide formation whilst the steel control sample, which was not connected to the photoanode, shows various phases of iron oxide lasts on it surface.



18.12 Raman spectra of the steel surface corroded in a 0.05 M  $K_2CO_3$  acidic solution. (a) under a continuously illuminated sample (30W lamp) and (b) a control sample not connected to the  $TiO_2$  photoanode. Figure adapted from Park *et al.* (2001).

## 18.5 Conclusion

It has been clearly demonstrated in this chapter that a simple TiO<sub>2</sub> photocatalytic coating can act as a photoanode in order to prevent metal corrosion. In conventional cathodic protection the sacrificial anode is either buried or immersed in the surrounding environment along with the metal structure requiring protection against corrosion and may need to be replaced regularly. Photoanodes allow for far easier maintenance. Moreover, even though the TiO<sub>2</sub> photoanode itself can be considered as a non-sacrificial material, the surrounding hole-scavenger medium is sacrificed over time due to its oxidation process that occurs in an irreversible path. This apparent drawback can be easily bypassed, however, through a low cost substitution of the hole-scavenging medium. From a practical application point of view, the use of a TiO<sub>2</sub> semiconductor material as a photoanode for metal cathodic protection has some limitations because it requires the presence of a UV light source. This limitation could be minimized, however, through the metal doping of the TiO<sub>2</sub> semiconductor material.

## 18.6 Future trends

One of the major challenges for the scientific and industrial community involved in research related to the application of TiO<sub>2</sub> as a photoanode for the prevention of metal corrosion is to increase its photo-sensitivity in the visible region of the electromagnetic spectrum. Future research strategies should be focused on this issue in order to obtain sustained photoactivity in the long run. The photoactivity of metal-doped TiO<sub>2</sub> under visible light should be attained through the development of new TiO<sub>2</sub> nanostructures with higher surface states, its doping with transition elements, the application of environmentally friendly and scalable production techniques or preparation methods (especially sol–gel-based ones) and new approaches to the incorporation of dopants in innovative TiO<sub>2</sub> nanostructures.

## 18.7 References

- Brinker, C.J. and Schere, G.W. (1990) *Sol–Gel Science: The Physics and Chemistry of Sol–Gel Processing*, Academic Press, New York.
- Carneiro, J.O., Teixeira, V., Portinha, A., Dupák, L., Magalhães, A. and Coutinho, P. (2005) ‘Study of the deposition parameters and Fe-dopant effect in the photocatalytic activity of TiO<sub>2</sub> films prepared by dc reactive magnetron sputtering’ *Vacuum*, **78**, 37–46. DOI: 10.1016/j.vacuum.2004.12.012
- Carneiro, J.O., Teixeira, V., Portinha, A., Magalhães, A., Coutinho, P., Tavares, C.J. and Newton, R. (2007) ‘Iron-doped photocatalytic TiO<sub>2</sub> sputtered coatings on plastics for self-cleaning applications’ *Mat. Sci. Eng. B*, **138**, 144–50. DOI: 10.1016/j.mseb.2005.08.130

- Carneiro, J.O., Teixeira, V., João, A., Magalhães, A. and Tavares, C.J. (2008) 'Study of Nd-doping effect and mechanical cracking on photoreactivity of TiO<sub>2</sub> thin films' *Vacuum*, **82**, 1475–81. DOI: 10.1016/j.vacuum.2008.03.013
- Carneiro, J.O., Teixeira, V., Carvalho, P., Azevedo, S. and Manninen, N. (2012) *Self-cleaning Smart Nanocoatings*, Woodhead Publishing Limited, Cambridge
- Cassie, A.B.D. and Baxter, S. (1944) 'Wettability of porous surfaces' *Trans Faraday Soc.*, **40**, 546–551. DOI: 10.1039/TF9444000546
- Challener, C. (2006) 'The intelligence behind smart coatings' *JCT Coatings Tech.*, www.coatingstech.org.
- Dickie, R. and Floyd, F.L. (1986) 'Polymeric materials for corrosion control: an overview' *ACS Symposium Series*, **322**, 1–16. DOI: 10.1021/bk-1986-0322.ch001
- Dong, Y., Bai, Z., Zhang, L., Liu, R. and Zhu, T. (2006) 'Finishing of cotton fabrics with aqueous nano-titanium dioxide dispersion and the decomposition of gaseous ammonia by ultraviolet irradiation' *J. Appl. Polymer. Sci.*, **99**, 286–91. DOI: 10.1002/app.22476
- Fei, B., Deng, Z., Xin, J.H., Zhang, Y. and Pang, G. (2006) 'Room temperature synthesis of rutile nanorods and their applications on cloth' *Nanotechnology* **17**, 1927–31. DOI:10.1088/0957-4484/17/8/021
- Fortunato, E., Ginley, D., Hosono, H. and Paine, D.C. (2007) 'Transparent conducting oxides for photovoltaics', *MRS Bull.*, **32**, 242–7. DOI:10.1557/mrs2007.29
- Fujishima, A. and Honda, K. (1972) 'Electrochemical photolysis of water at a semiconductor electrode' *Nature*, **238**, 37–8. DOI:10.1038/238037a0
- Fujishima, A., Hashimoto, K. and Watanabe, T. (1999) *TiO<sub>2</sub> Photo-catalysis. Fundamentals and Applications*, BKC, Tokyo.
- Furlong, D.N. and Sing, K.S.W. (1979) 'The precipitation of silica on titanium dioxide surfaces. I. Preparation of coated surfaces and examination by electrophoresis' *J. Colloid Interface Sci.*, **69**, 409–19. DOI: 10.1016/0021-9797(79)90130-9
- Gluszek, J., Jedrkowiak, J., Markowski, J. and Masal-ski, J. (1990) 'Galvanic couples of 316L steel with Ti and ion plated Ti and TiN coatings in Ringer's solutions' *Biomaterials*, **11**, 330–5. DOI: 10.1016/0142-9612(90)90109-4
- Grätzel, M. (2001) 'Photoelectrochemical cells' *Nature*, **414**, 338–44. DOI: 10.1038/35104607
- Grimes, C.A., Varghese, O.K. and Ranjan, S. (2007) *Light, Water, Hydrogen: The solar generation of hydrogen by water photoelectrolysis*, Springer, New York.
- Hashimoto, K., Irie, H. and Fujishima, A. (2005) 'TiO<sub>2</sub> Photocatalysis: a historical overview and future prospects' *Jpn. J. Appl. Phys.* **44**, 8269–85. DOI: 10.1143/JJAP.44.8269
- Hays, G.F. (2012) 'Now is the Time' World Corrosion Organization.
- Herbig, B. and Löbmann, P. (2004) 'TiO<sub>2</sub> photocatalysts deposited on fiber substrates by liquid phase deposition' *J. Photochem. Photobiol. A: Chem.* **163**, 359–65. DOI:10.1016/j.jphotochem.2004.01.005
- Hoffmann, M.R., Martin, S.T., Choi, W. and Bahnemann, D.W. (1995) 'Environmental applications of semiconductor photocatalysis' *Chem. Rev.*, **95**, 69–96. DOI:10.1021/cr00033a004
- Jones, D.A. (1996) *Principles and Prevention of Corrosion*, Prentice Hall, Englewood Cliffs NJ.
- Linsebigler, A.L., Lu, G. and Yates Jr, J.T. (1995) 'Photocatalysis on TiO<sub>2</sub> surfaces: principles, mechanisms, and selected results' *Chem. Rev.*, **95**, 735–58. DOI:10.1021/cr00035a013

- Liu, K. and Jiang, L. (2012) 'Bio-inspired self-cleaning surfaces' *Ann. Rev. Mat. Res.*, **42**, 231–63. DOI: 10.1146/annurev-matsci-070511-155046
- Moussa, S.O. and Hocking, M.G. (2001) 'The photo-inhibition of localized corrosion of 304 stainless steel in sodium chloride environment' *Corros. Sci.*, **43** (11), 2037–47. DOI: 10.1016/S0010-938X(01)00011-7
- NACE (2002), *Corrosion Costs and Preventive Strategies in U.S.*, Publication number FHWA-RD-01-156, US Department of Transportation.
- Nowotny, J., Sorrell, C.C., Sheppard, L.R. and Bak, T. (2005) 'Solar-hydrogen: Environmentally safe fuel for the future' *Int J Hydrogen Energy*, **30**, 521–44. DOI: 10.1016/j.ijhydene.2004.06.012
- Oblonsky, L.J. and Devine, T.M. (1995) 'Surface enhanced raman spectroscopic study of the passive films formed in borate buffer on iron, nickel, chromium and stainless steel', *Corros. Sci.*, **37**, 17–41. DOI: 10.1016/0010-938X(94)00102-C
- Ohko, Y., Saitoh, S., Tatsuma, T. and Fujishima, A. (2001) 'Photoelectrochemical anticorrosion and self-cleaning effects of a TiO<sub>2</sub> coating for type 304 stainless steel' *J. Electrochem. Soc.*, **148** (1), B24–8. DOI: 10.1149/1.1339030
- Park, H., Kim, K.Y. and Choi, W. (2001) 'A novel photoelectrochemical method of metal corrosion prevention using a TiO<sub>2</sub> solar panel' *Chem. Commun.*, 281–2. DOI: 10.1039/b008106j
- Perkgoz, N.K., Toru, R.S., Unal, E., Sefunc, M.A., Tek, S., Mutlugun, E., Soganci, I.M., Celiker, H., Celiker, G. and Demir, H.V. (2011) 'Photocatalytic hybrid nanocomposites of metal oxide nanoparticles enhanced towards the visible spectralrange' *Appl Catal B: Environ.*, **105**, 77–85. DOI: 10.1016/j.apcatb.2011.03.037
- Qi, K., Xin, J.H., Daoud, W.A. and Mak, C.L. (2007) 'Functionalizing polyester fiber with a self-cleaning property using anatase TiO<sub>2</sub> and low-temperature plasma treatment' *Int. J. App. Ceramic Technol.*, **4** (6), 554–63. DOI: 10.1111/j.1744-7402.2007.02168.x
- Quéré, D. (2008) 'Wetting and roughness' *Annu. Rev. Mater. Res.*, **38**, 71–99. DOI: 10.1146/annurev.matsci.38.060407.132434
- Reiche, P. (1950) *A Survey of Weathering Processes and Products*, University of New Mexico Press, Albuquerque, NM, 55.
- Serpone, N. (1995) 'Brief introductory remarks on heterogeneous photocatalysis' *Sol. Energ. Mat. Sol. Cells*, **38**, 369–79. DOI: 10.1016/0927-0248(94)00230-4
- Shanaghi, A., Sabour, A.R., Shahrabi, T. and Aliofkhazraee, M. (2009) 'Corrosion protection of mild steel by applying TiO<sub>2</sub> nanoparticle coating via sol–gel method' *Prot. Met. Phys. Chem. Surf.* **45** (3), 305–11. DOI: 10.1134/S2070205109030071
- Szymanowski, H., Sobczyk, A., Gazicki-Lipman, M., Jakubowski, W. and Klimek, L. (2005) 'Plasma enhanced CVD deposition of ritanium oxide for biomedical applications' *Surf. Coat. Technol.*, **200**, 1036.
- Teh, C.M. and Mohamed, A.R. (2011) 'Roles of TiO<sub>2</sub> and ion-doped TiO<sub>2</sub> on photocatalytic degradation of organic pollutants (phenolic compounds and dyes) in aqueous solutions: a review' *J. Alloys Compounds*, **509**, 1648–60. DOI: 10.1016/j.jallcom.2010.10.181
- Tung, W.S. and Daoud, W. (2009). 'Photocatalytic self-cleaning keratins: a visibility study' *Acta Biomater.*, **5**, 50–6. DOI: 10.1016/j.actbio.2008.08.009
- Uddin, M.J., Cesano, F., Bonino, F., Bordiga, S., Spoto, G., Scarano, D. and Zecchina, A. (2007) 'Photoactive TiO<sub>2</sub> films on cellulose fibres: synthesis and characterization' *J. Photochem. Photobiol. A: Chem.* **189**, 286–94. DOI: 10.1016/j.jphotochem.2007.02.015

- Vero, N., Hribernik, S., Andreozzi, P. and Sfligoj-Smole, M. (2009) 'Homogeneous self-cleaning coatings on cellulose materials derived from TIP/TiO<sub>2</sub> P25' *Fibers Polym.*, **10**, 716–23. DOI: 10.1007/s12221-010-0716-2
- Wei, Q., Yu, L., Mather, R.R. and Wang, X. (2007) 'Preparation and characterization of titanium dioxide nanocomposite fibers' *J. Mater. Sci.* **42**, 8001–5. DOI: 10.1007/s10853-007-1582-1
- Wenzel, R.N. (1936) 'Resistance of solid surfaces to wetting by water' *Ind. Eng. Chem.*, **28**, 988–94.
- Winkler, J. (2003) *Titanium Dioxide*, European Coatings Literature, Vincentz, Hannover.
- Xu, P., Liu, X., Wang, W. and Chen, S. (2006) 'Improving the antibacterial and UV-resistant properties of cotton by the titanium hydrosol treatment' *J. Appl. Polymer. Sci.* **102**, 1478–82. DOI: 10.1002/app.24340
- Xu, Y., Wu, N., Wei, Q. and Pi, X. (2008) 'Preparation and the light transmittance of TiO<sub>2</sub> deposited fabrics' *J. Coat. Technol. Res.*, **6** (4), 549–55. DOI: 10.1007/s11998-008-9149-x
- Young, T. (1805) 'An essay on the cohesion of fluids' *Philos. Trans. R. Soc. Lond.*, **95**, 65–87.
- Yuranova, T., Laub, D. and Kiwi, J. (2007) 'Synthesis, activity and characterization of textiles showing self-cleaning activity under daylight irradiation' *Catal. Today*, **122**, 109–17. DOI: 10.1016/j.cattod.2007.01.040